W boson mass in gauge-Higgs unification

Yuta Orikasa(CTU, IEAP)

Collaborator: Shuichiro Funatsu, Hisaki Hatanaka, Yutaka Hosotani, Naoki Yamatsu

Phys.Rev.D 108 (2023) 11, 115036

CDF anomaly

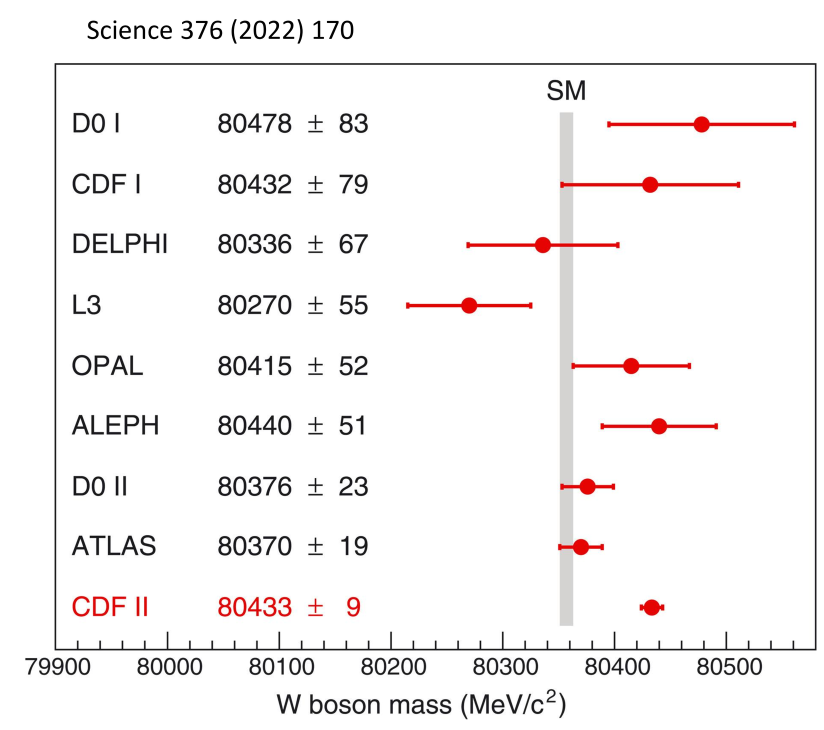

CDF has reported the anomaly of the W boson mass

SM : 80360 ± 7 MeV

CDF : 80433.5 ± 9.4 MeV

World average : 80369.2 ± 13.3 MeV

W boson mass was significantly higher than SM prediction with a discrepancy of 7 standard deviations.

Our result

80381 MeV < m_W^{GHU} <80407 MeV

for m_{KK}=13 TeV

SO(5) × U(1) gauge-Higgs Unification model in Randall-Sundrum space-time

Motivation

Higgs boson is a component of higher dimensional gauge boson ➔ Quadratic divergence is protected by gauge symmetry

Randall-Sundrum spacetime

Flat spacetime

- low KK mass scale : m_{kk}=600GeV
- Light Higgs boson : m_h=10 GeV

⇒Randall-Sundrum(RS) spacetime

Two branes and negative cosmological constant

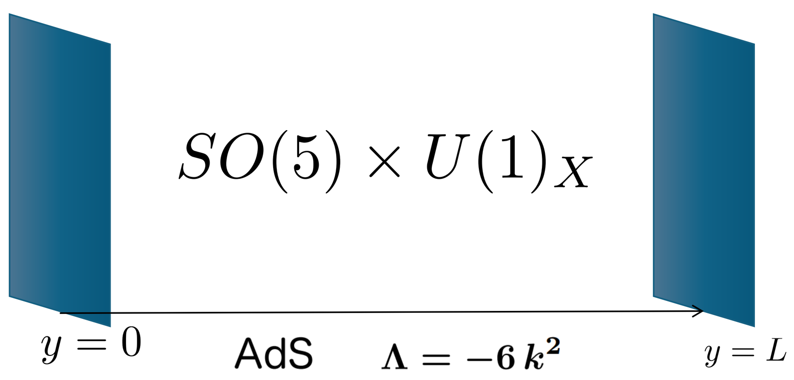

$$ds^2 = e^{-2k|y|}dx^\mu dx_\mu + dy^2$$

Kaluza-Klein mode

In higher dimensional theory, SM fields are expanded by Kaluza-Klein(KK) modes.
The typical mass scale is called KK mass scale:m_{kk}

Gauge symmetry

$SO(5) \times U(1)_X$

Boundary Condition

$$\to SO(4) \times U(1)_X \simeq SU(2)_R \times SU(2)_L \times U(1)_X$$

$$A_\mu(x,-y) = PA_\mu(x,y)P^{-1} \qquad A_y(x,-y) = -PA_y(x,y)P^{-1}$$
$$A_\mu(x,L-y) = PA_\mu(x,L+y)P^{-1} \qquad A_y(x,L-y) = -PA_y(x,L+y)P^{-1}$$

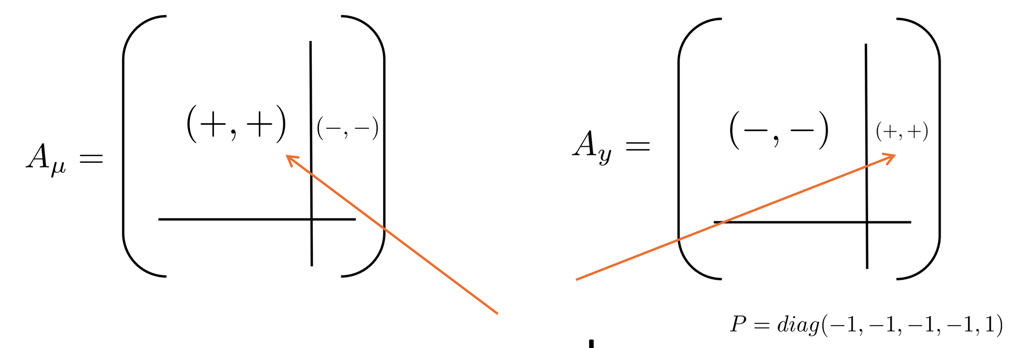

Brane scalar

$\to SU(2)_L \times U(1)_Y$ W_R, Z_R are massive

$$S^\Phi_{\rm brane} = \int d^5x\sqrt{-\det G}\,\delta(y)\Big\{ -(D_\mu\Phi_{(\mathbf{1},\mathbf{4})})^\dagger D^\mu\Phi_{(\mathbf{1},\mathbf{4})} - \lambda_{\Phi_{(\mathbf{1},\mathbf{4})}}\big(\Phi^\dagger_{(\mathbf{1},\mathbf{4})}\Phi_{(\mathbf{1},\mathbf{4})} - |w|^2\big)^2\Big\},$$

$$D_\mu\Phi_{(\mathbf{1},\mathbf{4})} = \Big\{\partial_\mu - ig_A\sum_{\alpha=1}^{10}A^\alpha_\mu T^\alpha - ig_B Q_X B_\mu\Big\}\Phi_{(\mathbf{1},\mathbf{4})} .$$

VEV of the brane scalar breaks SO(4) symmetry

Hosotani mechanism

$\to U(1)_{em}$ W, Z are massive

Wilson line phase θ_H is given by

$$exp\left(\frac{i}{2}\theta_H 2\sqrt{2}T^{\hat{4}}\right) = exp\left(ig_A\int_0^L dy\langle A_y\rangle\right)$$

$\theta_H \neq 0$ ➔ $SU(2)_L \times U(1)_Y \to U(1)_{EM}$

θ_H is a minimum of the effective potential

Particle contents

Field	G_{3221}	Left	Right	Name
$\Psi^\alpha_{(\mathbf{3},\mathbf{4})}$	$(\mathbf{3},\mathbf{2},\mathbf{1})_{\frac{1}{6}}$	$(+,+)$	$(-,-)$	u_j d_j
	$(\mathbf{3},\mathbf{1},\mathbf{2})_{\frac{1}{6}}$	$(-,-)$	$(+,+)$	u'_j d'_j
$\Psi^{\pm\alpha}_{(\mathbf{3},\mathbf{1})}$	$(\mathbf{3},\mathbf{1},\mathbf{1})_{-\frac{1}{3}}$	$(\pm,\pm)$	$(\mp,\mp)$	$D^\pm_j$
$\Psi^\alpha_{(\mathbf{1},\mathbf{4})}$	$(\mathbf{1},\mathbf{2},\mathbf{1})_{-\frac{1}{2}}$	$(+,+)$	$(-,-)$	ν_e e
	$(\mathbf{1},\mathbf{1},\mathbf{2})_{-\frac{1}{2}}$	$(-,-)$	$(+,+)$	ν'_e e'
Ψ_F	$(\mathbf{3},\mathbf{2},\mathbf{1})_{\frac{1}{6}}$	$(-,+)$	$(+,-)$	F_{1j} F_{2j}
	$(\mathbf{3},\mathbf{1},\mathbf{2})_{\frac{1}{6}}$	$(+,-)$	$(-,+)$	F'_{1j} F'_{2j}
$\Psi^{\pm\beta}_{(\mathbf{1},\mathbf{5})}$	$(\mathbf{1},\mathbf{2},\mathbf{2})_0$	$(\pm,\pm)$	$(\mp,\mp)$	$N^\pm$ $\hat{E}^\pm$ $E^\pm$ $\hat{N}^\pm$
	$(\mathbf{1},\mathbf{1},\mathbf{1})_0$	$(\mp,\mp)$	$(\pm,\pm)$	$S^\pm$
χ^α	$(\mathbf{1},\mathbf{1},\mathbf{1})_0$	…	…	χ
$\Phi_{(\mathbf{1},\mathbf{4})}$	$(\mathbf{1},\mathbf{2},\mathbf{1})_{\frac{1}{2}}$	…	…	$\Phi_{[\mathbf{2},\mathbf{1}]}$
	$(\mathbf{1},\mathbf{1},\mathbf{2})_{\frac{1}{2}}$	…	…	$\Phi_{[\mathbf{1},\mathbf{2}]}$

Gauge and Yukawa couplings

Gauge and Yukawa couplings are determined by the integration of fifth dimension

Table 2: The masses $m_{W^{(n)}}$ and couplings $\hat{g}^{W^{(n)}}_{e\nu_e,L}, \hat{g}^{W^{(n)}}_{\mu\nu_\mu,L}$ $(n = 0, 1, \cdots, 9)$ are shown for $m_{\rm KK} = 13$ TeV and $\theta_H = 0.10$ with $\sin^2\theta^0_W = 0.22266$. Right-handed couplings are very small; $|\hat{g}^{W^{(n)}}_{e\nu_e,R}| < 2\times10^{-20}$ and $|\hat{g}^{W^{(n)}}_{\mu\nu_\mu,R}| < 8\times10^{-19}$ for $n \le 14$.

n	$m_{W^{(n)}}$ [GeV]	$\frac{m_{W^{(n)}}}{m_{\rm KK}}$	$\frac{m_{W^{(0)}}}{m_{W^{(n)}}}$	$\hat{g}^{W^{(n)}}_{e\nu_e,L}$	$\hat{g}^{W^{(n)}}_{\mu\nu_\mu,L}$
0	80.396	0.0062	1	0.997649	0.997646
1	10199.	0.7845	7.88×10^{-3}	5.72126	5.44645
2	15857.	1.2198	5.07×10^{-3}	0.01858	0.01641
3	23102.	1.7771	3.48×10^{-3}	2.26066	1.72755
4	29032.	2.2332	2.77×10^{-3}	0.00607	0.00421
5	36074.	2.7749	2.23×10^{-3}	0.82175	0.59526
6	42099.	3.2384	1.91×10^{-3}	0.00291	0.00226
7	49062.	3.7740	1.64×10^{-3}	0.48331	0.36385
8	55135.	4.2412	1.46×10^{-3}	0.00173	0.00123
9	62056.	4.7735	1.30×10^{-3}	0.28815	0.20853

Free parameters

θ_H and m_{KK}

W boson mass

SM

Fermi constant determined from the μ-decay is given by

$$\frac{G_\mu}{\sqrt{2}} = \frac{\pi\alpha}{2s_W^2}\frac{1}{m_W^2}(1+\Delta r^{\rm loop}_{\rm SM}) ,$$

$$s_W^2 = 1 - \frac{m_W^2}{m_Z^2} ,$$

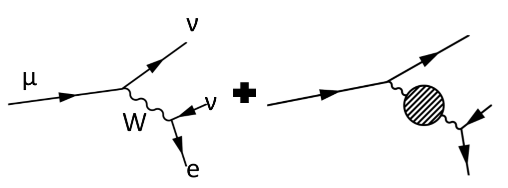

✚ Other loop contributions

$$m_W^{\rm SM} = \frac{m_Z}{\sqrt{2}}\left[1+\sqrt{1-\frac{4\pi\alpha(1+\Delta r^{\rm loop}_{\rm SM})}{\sqrt{2}\,G_\mu m_Z^2}}\,\right]^{1/2} .$$

$$\Delta r^{\rm loop}_{\rm SM} \simeq 0.0383 \pm 0.0004$$

GHU

Fermi constant in GHU includes tree and loop contributions

$$\frac{G_\mu}{\sqrt{2}} = \frac{\pi\alpha}{2\sin^2\theta^0_W}\frac{\hat{g}^{W^{(0)}}_{\mu\nu_\mu,L}\hat{g}^{W^{(0)}}_{e\nu_e,L}}{m^2_{W^{(0)}}}(1+\Delta r_G)(1+\Delta r^{\rm loop}_{\rm GHU}),$$

$$\Delta r_G = \frac{1}{\hat{g}^{W^{(0)}}_{\mu\nu_\mu,L}\hat{g}^{W^{(0)}}_{e\nu_e,L}}\sum_{n=1}^{\infty}\left\{\hat{g}^{W^{(n)}}_{\mu\nu_\mu,L}\hat{g}^{W^{(n)}}_{e\nu_e,L}\left[\frac{m_{W^{(0)}}}{m_{W^{(n)}}}\right]^2 + \hat{g}^{W_R^{(n)}}_{\mu\nu_\mu,L}\hat{g}^{W_R^{(n)}}_{e\nu_e,L}\left[\frac{m_{W^{(0)}}}{m_{W_R^{(n)}}}\right]^2\right\},$$

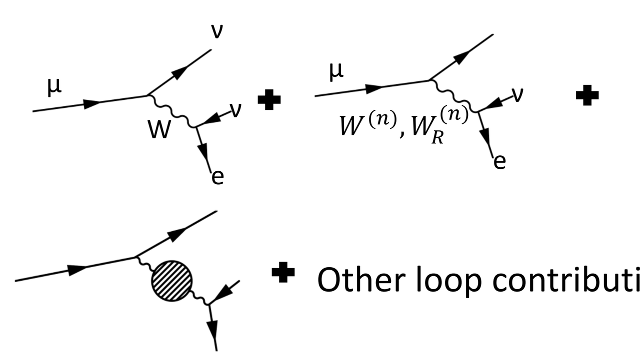

✚ Other loop contributions

We assume the loop contribution is the same as SM one and tree contribution is dominant.

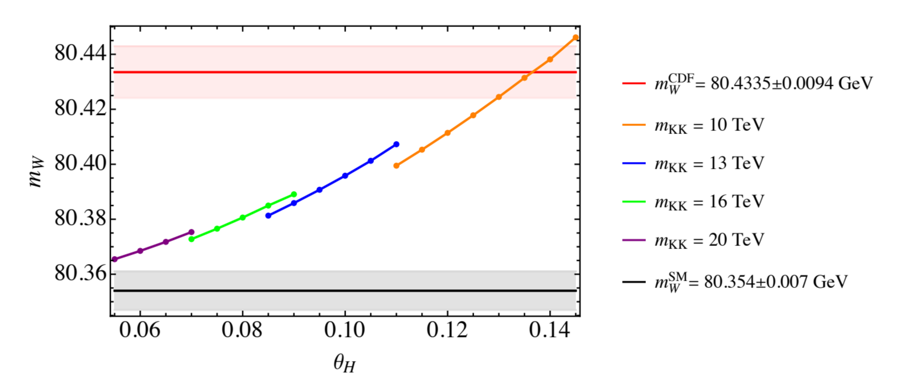

Figure 1: The W boson mass m_W in GHU is plotted as a function of θ_H with various $m_{\rm KK}$. The constraint $m_{\rm KK} \gtrsim 13$ TeV is obtained from the experimental data at LHC. [43] The predicted m_W in GHU for 13 TeV $\le m_{\rm KK} \le$ 20 TeV lies between $m_W^{\rm SM}$ and $m_W^{\rm CDF}$.

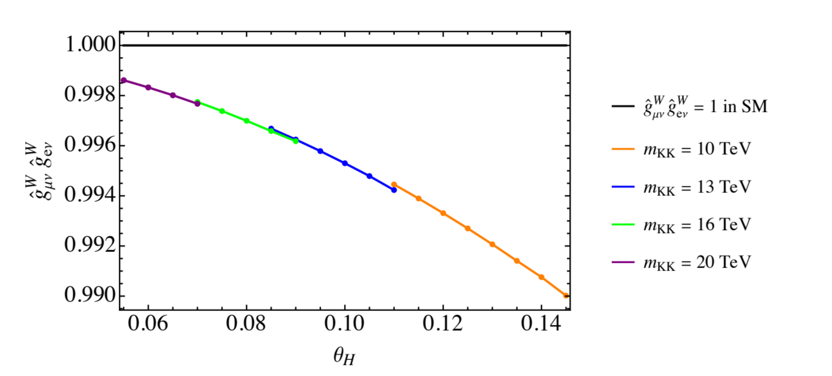

Figure 3: The product of the W couplings of μ and e normalized by the SM coupling $g_w/\sqrt{2}$, $\hat{g}^W_{\mu\nu}\hat{g}^W_{e\nu} \equiv \hat{g}^{W^{(0)}}_{\mu\nu_\mu,L}\hat{g}^{W^{(0)}}_{e\nu_e,L}$, is plotted as a function of θ_H with various $m_{\rm KK}$.

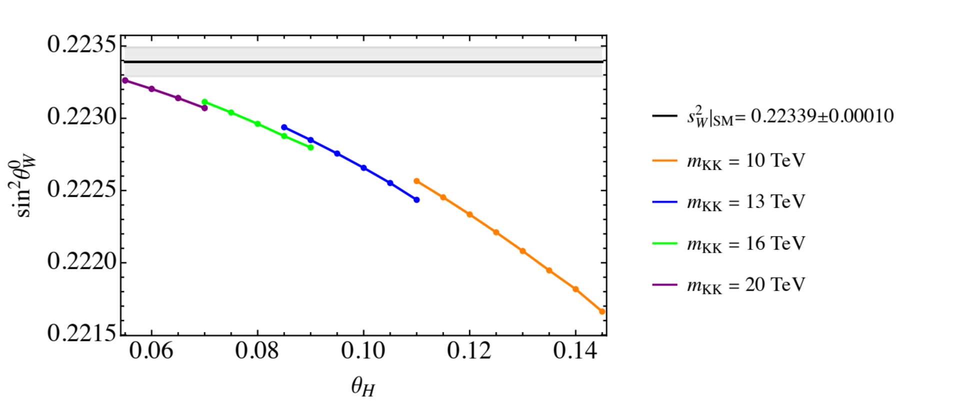

Figure 2: $\sin^2\theta^0_W$ in the on-shell scheme is plotted as a function of θ_H with various $m_{\rm KK}$. $s^2_W|_{\rm SM} = 1-(m_W^2/m_Z^2) = 0.22339 \pm 0.00010$ is the value in the on-shell scheme in the SM, listed in Table 10.2 of Ref. [49].

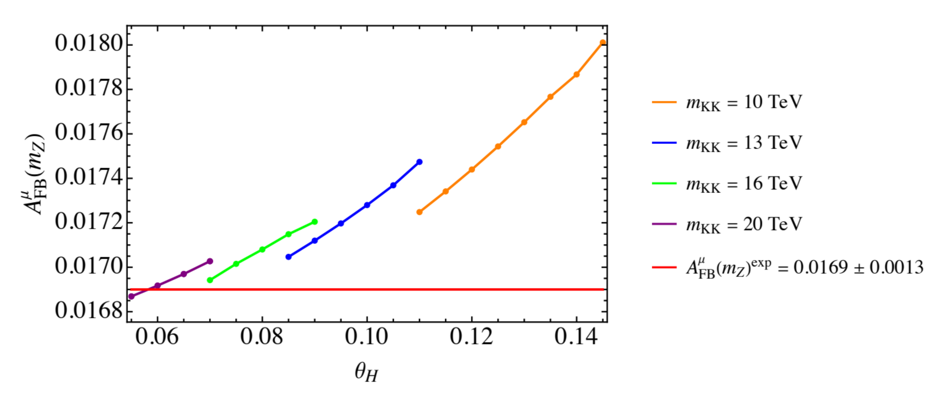

Figure 7: The forward-backward asymmetry in the process $e^-e^+ \to \mu^-\mu^+$ at the Z pole $A^\mu_{\rm FB}(m_Z)$ is plotted as a function of θ_H with various $m_{\rm KK}$. $A^\mu_{\rm FB}(m_Z)$ for 13 TeV $\le m_{\rm KK} \le$ 20 TeV is consistent with the observed value $A^\mu_{\rm FB}(m_Z)^{\rm exp} = 0.0169 \pm 0.0013$.